Calibration Approaches for Higher Order Ambisonic Microphones

Charles J Middlicott[1,2] and Bruce J Wiggins[1]

[1] *University of Derby, Derby, UK.* [2] *Sky Labs Brentwood, Essex, UK.*

Correspondence should be addressed to Charles J Middlicott
(charles@charlesmiddlicott.co.uk)

ABSTRACT

Recent years have seen an increase in the capture and production of ambisonic material due to companies such as YouTube and Facebook utilising ambisonics for spatial audio playback. Consequently, there is now a greater need for affordable high order microphone arrays due to this uptake in technology. This work details the development of a five-channel circular horizontal ambisonic microphone intended as a tool to explore various optimization techniques, focusing on capsule calibration & pre-processing approaches for unmatched capsule

1 Introduction

This paper expands on capsule calibration approaches utilised in our previous work [1], where a set of software tools were developed to aid ambisonic microphone array design and evaluation.

Typically, low cost microphone capsules are not mechanically matched at the production stage due to cost-effectiveness resulting in inconsistencies from capsule to capsule. This results in the user having to match them after the fact.

The capture of ambisonic signals was developed by Gerzon and Craven [2], where the notion of using a tetrahedral array of capsules was described. Various manufacturers have developed 1st order ambisonic (FOA) microphones based on the same design concepts such as those by Farrah [3], Core Sound [4] and Sennhiesser [5].

Users have been able to synthesize higher order ambisonic material in digital audio workstations (DAWs) for some time. However, the need for microphones capable of capturing such signals has recently grown due to increasing demand from content producers, as previously the use was confined to those in academic institutions. Commercially available arrays such as the mhAcoustics Eigenmike [6] are capable of capturing up to 4th order signals with CoreSound [7] and Brahma Microphones [8] having recently developed 2nd order arrays. Yet, these are out of reach of the everyday user due to the expensive nature of such high-quality arrays.

When considering the development of a low-cost alternative using inexpensive capsules for capturing ambisonic material, any deviation in the response between them will affect the quality of resulting the b-format signals. Due to the isotropic nature of ambisonics it is important that the capsule utilised have a uniformity between them so as to not colour or misrepresent the recorded sound-field.

Various approaches have been implemented in this paper to investigate how we can overcome the pitfalls of cheap unmatched capsules. The purpose of this work is to ascertain which capsule calibration approach is best utilised when working with low cost ambisonic microphones. At this stage no post-filtering of the B-Format signals has been investigated, this will be considered separately in a future paper.

Prototype array measurement has been undertaken and associated signal processing implemented to calibrate the individual microphone capsules. Details of the implementation can be seen in section 4.

The frequency response and directivity are shown at each stage of the process and this is compared to both simulations and the uncalibrated capsule responses. B-Format signals are generated from both the raw and calibrated capsule data as a means to evaluate the overall arrays performance.

2 Current Capsule Calibration Methods

Various approaches to capsule calibration for ambisonic microphones are utilised across both academic institutions and the commercial sector, due to the nature of the commercial market it has proven difficult to gather specifics on how manufacturers arrays are specifically calibrated.

Rode & Sennhiesser have a rich heritage in manufacturing microphones, the capsules both companies choose to use in their 1st order arrays are well matched in the first instance. Sennhiesser choose to forgo individual array measurement and capsule calibration opting to rely on the quality/matching of the capsules from the production line. They utilise generalised filtering in the supplied A/B conversion software to optimise the B-Format signals [9].

mhAcoustics also utilize well-matched capsules from Sennhiesser in the manufacture of the em32 array. Measurement of all the capsules characterise the array and additional calibration is implemented by applying individual capsule calibration weights using either of the supplied software packages eigenStudio & eigenSetGain [10].

Both the CoreSound TetraMic & OctaMic use well matched capsules and utilize a similar approach to mhAcoustics in that each array is individually characterised using a pseudo-anechoic measurement procedure to generate individualised array capsule calibration filters, these are applied by means of VST plugins VVEncode and VVOctoEncode. [11]. Brahma ambisonic microphones also use VVEncode to apply the individual array calibration filters. Angelo Farina has worked with Umashankar Manvathredi to generate A/B format matrices for the Bramaha microphones calibrating for microphone mismatch.

The SpHEAR* project is an array development study aimed at DIY ambisonics enthusiasts. Lopez-Lezcano' two papers on the project [12] and [13] discuss the capsule calibration and A/B conversion approaches for two microphone designs, a 1st order tetrahedral design and an eight capsule 2nd order design original proposed by Benjamin [14].

When calibrating the tetrahedral SpHEAR design in [12] Lopez opts to measure impulse responses of each capsule using 8 to 16 equally-spaced measurement points over the azimuth plane to compensate for the low frequency response of the capsules, differences in sensitivity and directivity, and the effects of the non-coincident nature of the array. When calibrating the 2nd order OctaThingy [13], Lopez notes the need for physically matched capsules due to differences in capsule gain and directivity causing errors in the recovery of the 2nd order harmonics. Stating that capsule equalisation by means of IR measurement will improve this recovery where the horizontal plane and low elevations are preferred for capsule calibration measurements as it is the most likely region of importance when recording with such a microphone.

Farina proposed an approach to capsule calibration for tetrahedral arrays in [15] as part of the A to B Format conversion process, where axial impulse response measurements of the capsules are taken these are used to generate filters by means of Nelson-Kirkeby inversion, where a measurement microphone is used as a reference. The authors have taken a similar approach to that of Farina regarding the measurement process and use of axial responses as a reference. The difference in our approach being that we opt for a theoretical flat response opposed to using a measurement microphone due to the obvious issues with alignment to the prototype array.

Adriensen developed a suite of software called TetraProc and TetraCal [16], An ambisonic microphone processor and calibration tool. TetraProc splits into three sections, compensating from any mismatch in sensitivity and directivity, equalisation to compensate for the non-coincident nature of the array at mid to high frequencies and finally compensation in the LF region to correct for the high-pass nature of directional microphones. This calibration tool takes eight 45˚ impulse response measurements in the azimuth plane to compensate solely for deviation in capsule sensitivity & directivity, additional the speaker response is measured so that it can be compensated for, A similar approach is taken in this work, but measurements are captured at a higher resolution.

3 Prototype Array Development

3.1 Array Design Considerations

A cost-effective 2nd order horizontal Ambisonic microphone prototype has been developed as a vehicle to evaluate several approaches to higher order array calibration. It can be shown that the minimum number of capsules needed to capture the horizontal only 2nd order spherical harmonics using an equal angle sampling distribution is 2N+1, where N is the order [17]. This leads to an initial circular array prototype that consists of five 14mm electret capsules with a capsule spacing of 72° and an array radius of 25mm. This radius was calculated taking into account the physical size of the JLI 140A-T capsules utilized [18]. Figure 1 below shows the array geometry & housing designed in SolidWorks. It was decided to focus initially on an increased resolution in the azimuth plane. Factors such as spacing, calibration and filtering could then be evaluated with greater ease with findings informing the development of a 3D spherical array.

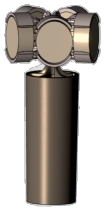

Figure 1 – Five Channel 3D Printed Housing in SolidWorks

3.2 Objective Measurement Process

Objective measurement took place in a hemi-anechoic chamber, a set of measured impulse responses (IRs) were captured at 2-degree increments along the azimuth plane, from an on-axis position to 180 degrees above which symmetry was assumed. To both further the accuracy and minimize the length of the measurement process, an Outline ET250-3D [19] automated turntable was utilized. Measurements were taken at a 2 metre distance from the acoustic centre of the capsules under test. A total set of 450 measured IRs were captured.

The measurement source material was a 15 second 20Hz to 20kHz logarithmic sine sweep, this was fed to a DynAudio BX5a loudspeaker. An omnidirectional Earthworks measurement microphone [20] was used to capture the response of the loudspeaker. Nelson/Kirkeby inversion [21] was utilized to generate an inverse of this speaker response shown in Figure 2 using Eq. 4 . The resultant filter is convolved with the captured IRs thus compensating for the frequency response of the loudspeaker.

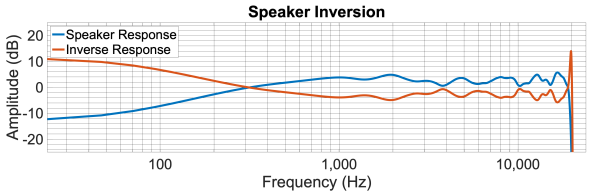

Figure 2 - Speaker / Inverse Filter in the Frequency Domain

3.3 Raw Measured Responses

To evaluate the feasibility of using these capsules within a prototype ambisonic array, the deviation in frequency evident between the five capsules on-axis responses was considered. This was to ascertain how matched the capsules were from the production line. The initial on-axis response measurements show a deviation of approximately +/- 1.5dB between 50Hz and 6.5kHz, above which the deviation increases to +/- 2dB and the sensitivity ranges quite significantly between the capsules above this frequency. This can be below shown in Figure 3.

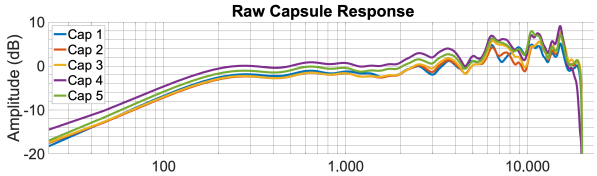

Figure 3 - Measured On-Axis Capsule Frequency Response

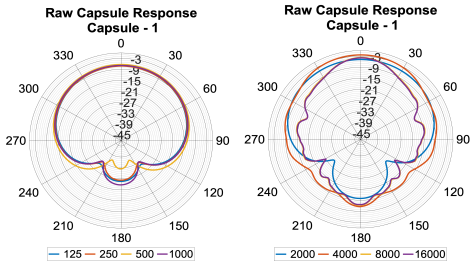

Figure 4 - Polar Response of Capsule 1

The raw capsule directivity shown above in Figure 4 exhibits a cardioid like response up to 1kHz, at 2kHz the response mirrors more of a super-cardioid pattern as shown by the -15dB figure at 180˚ this is opposed to -27 to -33dB below 1kHz.

The higher frequency regions of 8kHz and above exhibit an increase in directivity response, albeit not as smooth as with the lower frequencies, this can be attributed to the design of the capsules housing.

The remaining four capsules exhibit a similar response as above, where at frequencies below 6kHz they are within a +/- 1.5dB range. Above 6kHz the responses deviate from capsule to capsule quite dramatically. This can be seen for on axis positions in Figure 3. Additional polar responses for the remaining capsules can be reviewed in an appendix available online [22].

4 HOA Microphone Array Calibration Approaches & Implementation

Due to the low cost per unit of the capsules utilised, matching at the production stage isn't a viable option. Thus, we must develop an approach to calibrate the capsules that culminates in a desired matched response for all transducers within an array. In the following section, four approaches to capsule calibration are investigated for use with Ambisonic microphone arrays.

4.1 Calibration by 1/3rd Octave Average Gain Matching

The first method considered utilizes gain matching of the capsules within an array. This is arguably the simplest of the approaches being evaluated, in that some form of gain or attenuation is applied to each transducer to level match the signals.

Gain matching of the capsules could be implemented using only this time domain signals as a reference, however this has no dependency on the frequency response of the capsules. To successfully gain match these capsules it was deemed necessary to analyze each capsules response in the frequency domain by apply a Fast Fourier Transform (FFT) to each capsules on-axis impulse response.

To increase the flexibility of this method the authors chose to average over 1/3rd octave bands instead of over all frequencies. This was so that some of the octaves can be omitted when generating the correction factor at the discretion of the operator. thus, gain matching for a frequency range of interest.

The equations 1 & 2 below show how the frequency index ***(k),*** which corresponds to the upper and lower limits of each 1/3rd octave band were calculated. Respective of the size of the FFT being applied which was 2048 points.

$$UpLim_{(k)} = \frac{F_{max}}{Fs/FFTSize} \quad (1)$$

$$LoLim_{(k)} = \frac{F_{min}}{F_s/FFT_{Size}} \quad (2)$$

Where

$\boldsymbol{F_{max}}$ = Upper 1/3rd Oct. Frequency Limit in Hz
$\boldsymbol{F_{min}}$ = Lower 1/3rd Oct. Frequency Limit in Hz
$\boldsymbol{F_s}$ = Sampling Frequency (48_{kHz})
$\boldsymbol{FFT_{Size}}$ = Length of the FFT to be applied (2048)

Once the frequency indices for each set of octave limits, are calculated the magnitude of the capsules on-axis response is averaged per each 1/3rd octave band. This is shown in equation 3 below.

$$1/3rd\ Oct\ Avg_{(c,k)} = \frac{1}{UpLim_{(k)} - LoLim_{(k)}} \sum_{LoLim_{(k)}}^{UpLim_{(k)}} \left|FFT_{(c)}\right| \quad (3)$$

Where

$\boldsymbol{c}$ = Capsule Index
$\boldsymbol{k}$ = Frequency Index
$\boldsymbol{UpLim_{(k)}}$ = Upper Limit Index Per Octave
$\boldsymbol{LoLim_{(k)}}$ = Lower Limit Index Per Octave
$\boldsymbol{FFT_{(c)}}$ = On Axis FFT Data for Capsule (c)

Once each capsules response has been averaged. The mean per capsule is used to generate a correction factor. This is achieved by taking the lowest mean figure as a reference. Applying attenuation to the remaining capsules relative to the difference between each capsule and the reference.

The authors opted to use the lowest capsules average magnitude as a reference, so as to not add any excess gain preferring to match by attenuation. The result of this attenuation is shown in Figure 5**.**

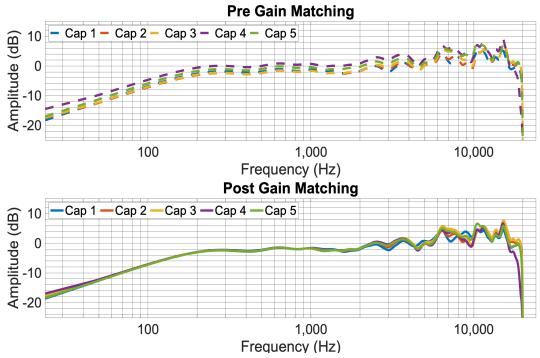

Figure 5 – On Axis Response (Pre/Post Gain Matching)

4.2 Calibration to a Specific Capsules On-Axis Frequency Response

The following approach matches all the capsules within an array to whichever capsules axial frequency response is deemed more desirable by the user.

This target response is ascertained by observing the axial frequency response each capsule. Once a target response is chosen it is used in conjunction with the remaining axial responses to invert between one another resulting in an inverse filter which can be calculated using the following equation.

$$H_{inv}(\mathrm{k}) = \frac{H_{Target}(k) \cdot Conj(H(k))}{Conj(H(k)) \cdot H(k) + \epsilon(k)} \qquad (4)$$

Where $\boldsymbol{H(k)}$ is the measured response, $\boldsymbol{H_{Target(k)}}$ is the desired target response, $\boldsymbol{\epsilon(k)}$ *is* the frequency dependent regularisation parameter and $\mathbf{k}$ is the frequency index. The generated filters are then convolved with its respective measured response so as to exhibit a close approximation to the desired target response.

Frequency dependent regularisation $\boldsymbol{\epsilon(k)}$ was used throughout this work, as to not generate large increases at the extremities of the frequency range of interest. four points were chosen at which the regularisation figure would change. The limits were set as follows, 20Hz and 200Hz for the lower frequency region and 8kHz and 16kHz for the higher frequency region. Between the inner limits (200Hz - 8kHz) the regularisation parameter was set a 0.01, outside of which the regularisation was set to 1. Between these inner and outer limits (20Hz to 200Hz and 8kHz to 16kHz) the regularisation parameter decreased in the LF region from 1 to 0.01 in a linear fashion and increased from 0.01 to 1 in the HF region as shown below in Figure 6.

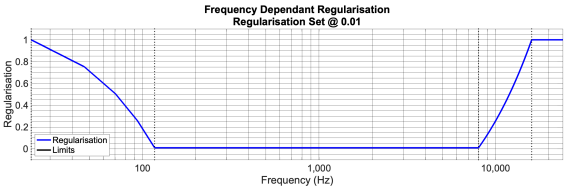

Figure 6 – Frequency Dependent Regularization

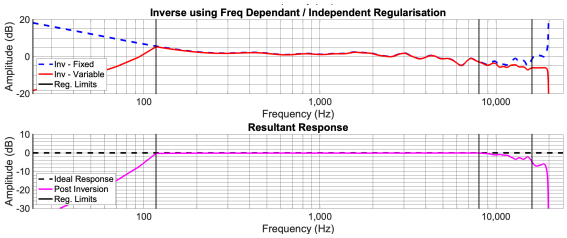

Figure 7 – Effect of Using Frequency Dependent vs. Frequency Independent Regularization

Figure 7 illustrates the effect of using frequency dependent regularisation over a fixed frequency independent approach. The trace showing a blue dotted line is the calculated inverse filter using frequency independent regularisation of 0.01. In can be shown that this would result in a large increase of ~20dB at 20Hz and a similar increase at 16kHz. The red trace shows the effect of using frequency dependent regularisation where it is evident that the linear change in value positively impacts the result of the invert filter. The lower of the two axes shows the result of applying both regularisation approaches. The frequency independent approach results in a flat response over 20Hz/20kHz at the expense of excessive increases in the LF/HF range due to the ill-conditioned nature of the filters. The pink trace shows the result of using frequency dependent regularisation, where a flat response is evident between the inner frequency limits (200Hz to 8kHz), outside of which there is a roll off evident, showing no excessive increase in the extremities.

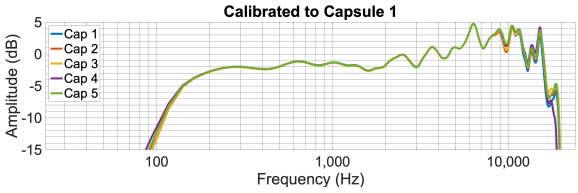

Figure 8 - Calibrated to a Capsules Axial Response

The resultant axial frequency response is shown above in Figure 8, where between the inner regularisation limits of (200Hz - 8kHz) the target response is achieved. The LF/HF roll-off can be attributed to using frequency dependent regularisation which causes some differences to that of the target response in this region.

4.3 Calibration to a Flat Frequency Response

The third calibration approach investigated is one in which the capsules are calibrated to a flat frequency response. This is achieved by the on axis measured responses being inverted as in equation **(1)** to a target that is a Dirac's delta function **δ** opposed to an optimal measured response shown in section ***4.2***.

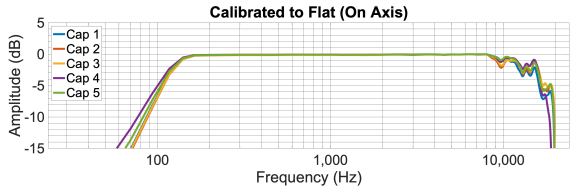

Figure 9 – Calibrating to a Flat On-Axis Response with Frequency Dependent Regularization

The resultant axial frequency response of each capsule is shown above in Figure 9, where a flat frequency response is evident between 120Hz/8kHz. The LF/HF roll-off can be attributed to using frequency dependent regularisation.

4.4 Calibration by Diffuse Field Equalization

The final approach implemented in this work utilizes diffuse field equalization. Approximation of the average diffuse field response is calculated by using a large set of measured free-field responses taken from the measurement procedure outlined in section 3.2. The inverse of this response is used as a target in which individual calibration filters are generated. Averaging the array response over a diffuse field, rather than relying on a single on axis free-field response for calibration. The averaged diffuse-field calculation is shown in Equation 5. A similar approach was taken by Heller [23] for the post filtering of 1st order ambisonic components.

$$\mathrm{DFR(c)} = \sqrt{\frac{1}{D}\sum_{d=1}^{D}\left|FFT_{(c,d,k)}\right|^2} \qquad (5)$$

Where

$\boldsymbol{D}$ = Number of Measurement Directions
$\boldsymbol{d}$ = Measurement Position Index (1 to D).
$\boldsymbol{c}$ = Capsule Index
$\boldsymbol{k}$ = Frequency Index of FFT
$\boldsymbol{FFT}_{(c,d,k)}$ = FFT of Measured Responses

The calculated diffuse-field responses are shown in Figure 10 below. The inverse of which is applied to the measured responses the resulting in the axial responses shown in Figure 11.

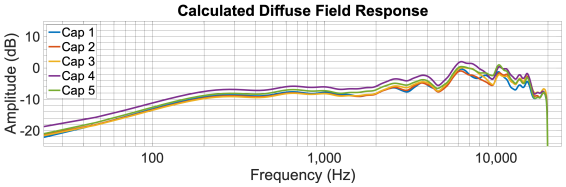

Figure 10 – Calculated Diffuse Field Response

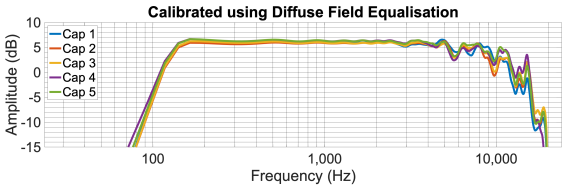

Figure 11 – Calibrating with Diffuse Field Equalization

5 Microphone Array Simulation

A simulation routine developed previously in [1] was used to derive a theoretical response, mirroring the characteristics of an array in anechoic conditions. The cardioid directivity response of each capsule is shown in Figure 12.

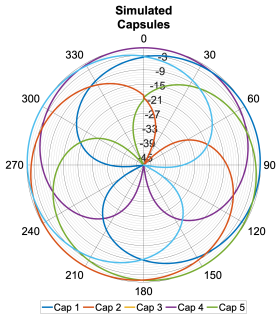

Figure 12 – Directivity of the Simulated Five Channel Array

5.1 Generating Spherical Harmonics

To accurately assess the performance of the prefiltering methods considered in this paper, it was critical that we evaluate the prototype arrays response in the spherical harmonic domain.

Figure 13 shows the ideal response of the spherical harmonics (SH) needed to derive 2nd order ambisonics. In this case the minimum number of harmonics is five (2N+1). The ambisonic channel number (ACN) naming convention is used throughout this work and the directivity in the azimuth plane can be seen below.

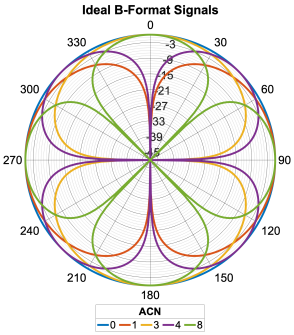

Figure 13 - Ideal Harmonics (2nd Order Horizontal)

To generate the desired B-Format signals a set of SH coefficients must be calculated and applied to each microphone capsule. The coefficients for each SH are generated using the following equation, modified from [24].

$$Y_n^m(\theta,\phi) \equiv N_n^{|m|} P_n^{|m|}(\sin(M_\phi)) \begin{Bmatrix} \cos(|m|M_\theta) & \text{if } m \geq 0 \\ \sin(|m|M_\theta) & \text{if } m < 0 \end{Bmatrix} \quad (6)$$

Where

M_θ	= The angular capsule azimuth in radians	
M_Φ	= The angular capsule elevation in radians	
n	= The order	(0 to the max order *N*)
m	= The degree	(-*n* to *n*)
P_n^m	= The associated Legendre polynomial	
N_n^m	= Gain value for a given normalisation scheme	

Once calculated for a given SH they must be convolved with each respective capsules IRs. These are then summed together to create the desired SH signal.

The simulated B-Format Signals for Ambisonic Channel Number (ACN) 3 & 4 and shown below in Figure 14.

It should be explicitly noted that no post-filtering has been applied to the B-Format Signals at this stage as the purpose of this work is to focus solely on capsule pre-filtering strategies.

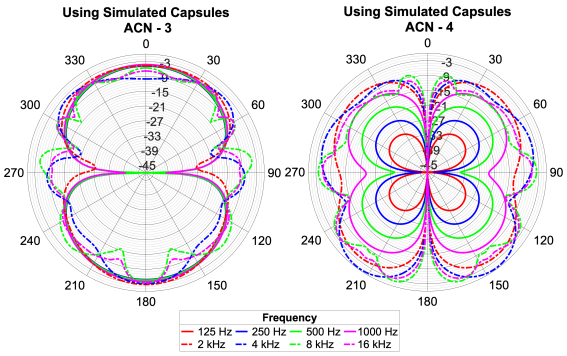

Figure 14 - Simulated B-Format Signals (ACN 3 & ACN 4)

When comparing the ideal harmonics against its simulated counterpart, (which use perfect cardioid responses) It can be observed that several factors affect the array response, most notably the non-coincident nature of the array at higher frequencies. This is a direct consequence of the array design, where the radius (25mm) and capsule spacing (72˚) cause the array response to deteriorate above a specific frequency. Above which the directivity is skewed to the individual capsules look direction. This is known as the spatial aliasing frequency, this begins to affect the array response above 4.3kHz. This is approximated below by using equation 7.

$$\text{Aliasing Frequency} = \frac{Nc}{2\pi r} \quad (7)$$

Where

N	= Is the Ambisonic Order	(2nd Order)
c	= Speed of Sound	(343m/s)
r	= Is the Array Radius	(25mm)

Due to the above, in the remaining figures the array responses will be shown up to 4kHz only, as the scope of this paper isn't to consider post filtering.

6 Evaluation of Calibration Approaches

To accurately assess the performance of each calibration method implemented, the following section considers both the calibrated capsule directivity and the directivity of the generated B-Format signals for each approach investigated. These are compared to both simulated and raw measured responses for analysis. Additional results and figures for all capsules and B-Format responses not included in this paper, are freely available in appendix online [22].

The ideal & simulated B-Format responses are considered when evaluating the performance of the calibration approaches. However, the raw measured directivity of each capsule differs quite drastically from a perfect cardioid response at HF. Thus, the B-Format responses generated would typically suffer. Due to this the authors have chosen to display the raw B-Format signals as a benchmark on which to assess the difference between the calibration approaches.

6.1 Raw Measured B-Format Responses

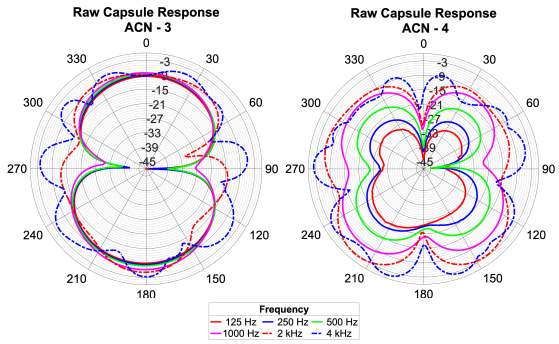

Figure 15 – Raw Measured B-Format Signals

ACN 3 response shown in Figure 15 mirrors the simulated response in Figure 14 up to 500Hz where the null at 1kHz (90˚) deviates by 12dB, above this frequency the response deteriorates. The response of ACN 4 in comparison tracks below 1kHz with a distinct exception between 180˚/270˚ where the expected nulls in the pattern as per the simulation are non-existent and the directivity deteriorates.

6.2 Calibration by Avg. Gain Matching

Averaged gain matching is the simplest of the methods considered in this paper, due to attenuation of the capsules input signals instead of filtering in the frequency domain. The directivity response over the five capsules shows no obvious difference the raw directivity responses aside from a minor change in gain, this can be seen for the axial positions in Figure 5.

In the SH domain, shown in Figure 16, ACN 3 loosely mirrors the ideal response up to 1kHz above which it deteriorates. The directivity of ACN 4 mirrors its simulated counterpart below 500Hz where a decrease of ~6dB per octave is observed due to the size of the array and the directional nature of the capsules. A slight improvement is observed at 270˚ when compared to the Raw ACN 3 response at 1kHz in Figure 15. However, ACN 4 shows a vast improvement below 1kHz between 180˚/270˚ where the accuracy of the derived pattern improves compared to the raw response mirroring the simulation, at 2kHz the nulls are more prominent at both 0˚ and 180˚.

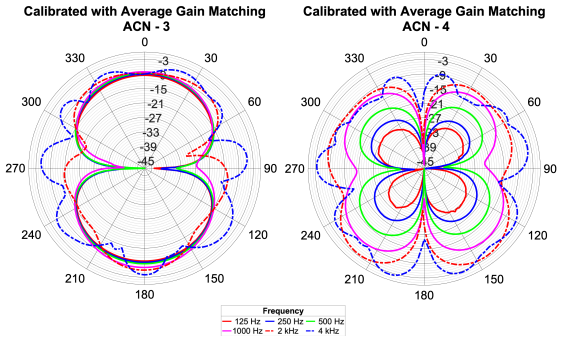

Figure 16 – Gain Matched B-Format Signals

6.3 Calibration to a Specific Capsules On-Axis Frequency Response

When matching the 2nd capsules axial response to the target response of capsule one it reaches the desired response for the on-axis position (0˚ and 72˚ respectively). this is shown in Figure . Both capsules two and three exhibit a minor increase in gain of about 1dB whereas capsules four and five exhibit a decrease of about 2dB and 1dB respectively in comparison to the raw directivity. This can be observed by comparing the axial responses from Figure 3 with the responses in Figure 8. When considering the HF region of 8kHz and above there is a decrease of ~2dB from the target response across all capsules due to the effect of the frequency dependent regularization.

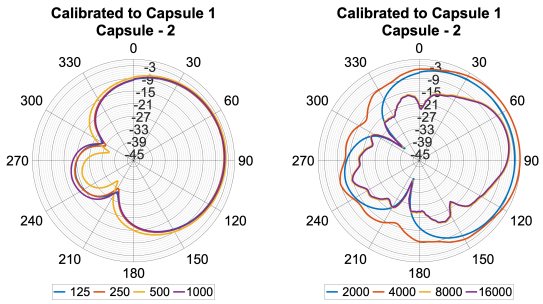

Figure 17 – Capsule 2 Calibrated to Capsule 1 On-Axis

ACN 3 in Figure 18 loosely mirrors both the ideal and simulated responses up to 250Hz, above which it the response deteriorates. The directivity of ACN 4 exhibits the ~6dB per octave decrease at 1kHz in line with the simulated directivity response where the cardinal direction is observed.

Comparing ACN 3 to the raw response the nulls at 500Hz are less pronounced and at 1kHz severe deterioration at both 90˚ and 270˚ is evident where a null is typically expected. Below 500Hz ACN 4 exhibits more pronounced nulls than the raw response and the directivity in Figure 16 is skewed between 0˚/90˚ with ~4dB decrease in sensitivity at the cardinal direction.

Both calibration methods tested so far have successfully derived a more accurate directivity pattern between 180˚ and 270˚ when comparing the raw ACN 4 response, in this implementation the directivity lacks consistency at 45˚ below 1kHz due to a decrease in sensitivity. ACN 3 exhibits a similar directivity in the cardinal direction but suffers due to the decrease or lack of nulls at 90˚/270˚ respectively.

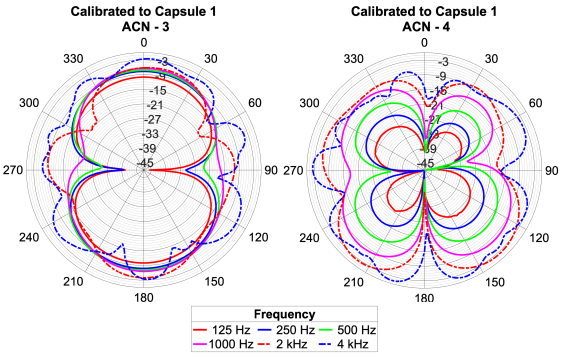

Figure 18 – B-Format Signals Calibrated to Capsule 1

6.4 Calibration to a Flat On-Axis Response

Calibration to a flat axial response has shown to exhibit the smallest deviation between capsules thus far, below 8kHz the axial response matches the target as desired, with a minus 3dB beam width of +/- 30˚. Again, as a product of the regularization used, above 8kHz a decrease in magnitude of ~4-5dB from a theoretical flat response is observed in Figure 19.

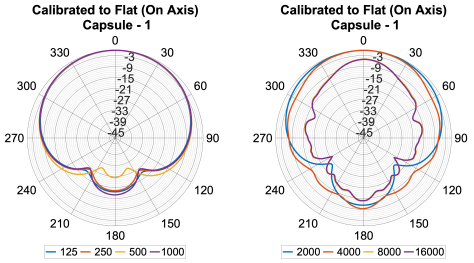

Figure 19 – Calibrated to a Flat On-Axis Response

This translates to the SH domain in a very similar manner as in the previous calibration approach. It can be observed when comparing Figures 18 and 20 that in both cases ACN 3 exhibits poor attenuation at the null directions at 1kHz, potentially due to the fact that this calibration method optimised for the capsules axial positions, this results a directivity that is less desirable than the raw B-Format response.

Although ACN 4 exhibits a more desirable response than its uncalibrated counterpart, the same issues arise as with the last calibration method where at the cardinal direction between 0˚ to 90˚ the response in decreases in amplitude by ~6dB at 500Hz and below thus skewing the directivity.

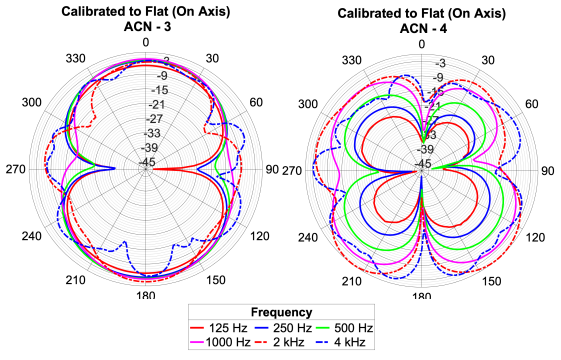

Figure 20 – B-Format Signals Calibrated to Flat (On-Axis)

6.5 Calibration by Diffuse Field Equalization

Previous approaches optimize based on axial responses, these have shown to have a negative impact for off-axis positions in some cases, see Figures 18 and 20. Averaging over the diffuse-field attempts to negates this issue by having no bias on a specific angle of incidence. From a capsule perspective this has shown to offer a near flat response below 4kHz at the axial position but above 8kHz exhibits a roll-off where frequency deviation is evident, see Figure 11. This calibration approach resulted in a slight decrease in the directionality of the polar responses, exhibiting a more sub-cardioid directivity at lower frequencies compared to the uncalibrated capsules This can be confirmed by observing the directivity responses in Figure 21.

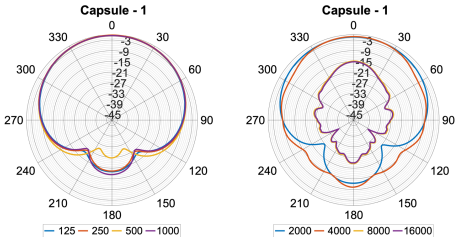

Figure 21 – Calibrated Using Diffuse Field Equalization

Of the approaches implemented in this paper, diffuse-field equalization yields the most accurate B-Format responses in respect to the simulated counterpart, nulls in both responses shown in Figure 22 are largely improved over the raw measured responses and there is greater consistency in the cardinal directions in comparison to the previous calibration approaches.

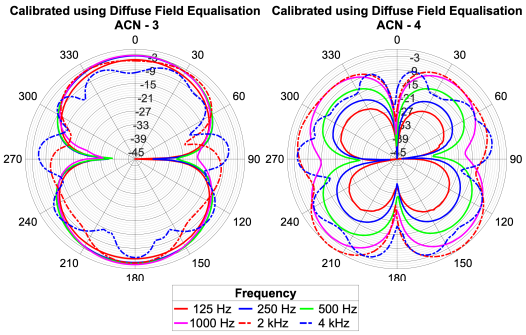

Figure 22 – Diffuse Field Equalized B-Format Signals

7 Future Work

Research results show some interesting points regarding capsule calibration and optimization approaches, leaning towards optimizing with no bias to one particular angle of incidence, as opposed to an on-axis based approach. these approaches also highlight the importance of effective pre and post-filtering.

The work conducted has shown scope for further investigation; specifically, the expansion to include the full 3D spherical arrays. Consequently, development of several array prototypes is under construction and these prototypes will be measured imminently, including an investigation into the generation of B-Format signals and associated post filtering approaches.

Worthy of notation the microphone array simulation routine utilized in this work, although useful, would benefit from additional features such as frequency dependent capsule directivity, along with the updates to the associated applications [1].

8 Conclusions

The implementation of several capsule calibration approaches for ambisonic microphone arrays has been outlined and evaluated. Analysis of the array response at each stage of the calibration process has shown that when calibrating with inexpensive microphone capsules all of the approaches considered in this paper have offered some degree of improvement upon the raw B-Format, but when the calibration approach optimizes for an axial capsule response a correlation between this dependency on a fixed angle and the deterioration of the B-Format directivity response at certain off-axis angles is evident. When an approach such as Average Gain Matching or Diffuse Field Equalisation is utilised the resultant array response observed exhibits a more robust B-Format directivity than if optimising for an axial position by filtering in the frequency domain. It should be noted, the ability to accurately derive the desired directivity above 2kHz has continually been sub-optimal regardless of the approach used, this re-affirms the need for effective post-filtering when calibrating ambisonic microphones, especially when using low cost capsules.

References

[1] Middlicott C; Wiggins B; Development of Ambisonic Microphone Design Tools—Part 1 In Audio Engineering Society Convention 145, eBrief - 489, 2018.

[2] Gerzon M. A, Craven P, “Coincident Microphone Simulation Covering Three Dimensional Space and Yielding Various Directional Outputs” 1977.

[3] Farrar. K, “Soundfield Microphone: Design and Development of a Microphone and Control Unit” 1979.

[4] CoreSound LLC; TetraMic Microphone, http://www.core-sound.com/TetraMic/1.php

[5] Sennhiesser GmbH; Ambeo VR Mic, https://en.uk.sennheiser.com/microphone-3d-audio-ambeo-vrmic

[6] mhAcoustics LLC; EigenMike32 http://www.mhacoustics.com

[7] CoreSound LLC; OctoMic Microphone http://www.core-sound.com/OctoMic/1.php

[8] Manvathredi U; Brahma Microphones http://www.brahamamics.com

[9] Sennhiesser Electronic GmbH, A to B Format Conversion Software http://www.sennheiser-sites.com/responsive-manuals/AMBEO_VR_MIC/EN/index.html#page/AMBEO_VR_MIC_EN%2FVR_MIC_04_Software_EN.4.1.html%23ww1016646

[10] mhAcoustics LLC, SetGain Application User Manual (Capsule Calibration Process) https://mhacoustics.com/sites/default/files/em32setGain%20User%20Manual%20R01A.pdf

[11] VVAudio, VVEncode / VVOctoEncode (For CoreSound/Brahma Calibration Filters) https://www.vvaudio.com/products/VVEncode https://www.vvaudio.com/products/VVOctoEncode

[12] Lopez-Lezcano, F; The *Sphear Project, A Family Of Parametric 3D Printed Soundfield Microphone Arrays, In Audio Engineering Society Conference on Soundfield Control, 2016.

[13] Lopez-Lezcano, F; The *SpHEAR project update: the TinySpHEAR and Octathingy soundfield microphones, In Audio Engineering Society Conference on Audio for Virtual and Augmented Reality, 2018.

[14] Benjamin, E; A Second-Order Soundfield Microphone with Improved Polar Pattern Shape, In Audio Engineering Society Convention 133, Convention Paper - 8728, 2012.

[15] Farina, A; A2B Conversion – Oct 2006 http://pcfarina.eng.unipr.it/Public/B-format/A2B-conversion/A2B.htm

[16] Adriensen, F; A Tetrahedral Microphone Processor for Ambisonic Recording https://kokkinizita.linuxaudio.org/papers/tetraproc.pdf

[17] Rafaely, B; Fundamentals of Spherical Array Processing, Topics in Signal Processing, Vol 8 – Springer Verlag, Berlin (2015) DOI 10.1007/978-3-662-45664-4

[18] JLI Electronics LLC, JLI140A-T Electret http://www.jlielectronics.com/content/JLI-140A-T.pdf

[19] Outline – ET250-3D Automated Turntable https://outline.it/outline-products/measurement-systems/et-250-3d/

[20] Earthworks Inc. "M30BX Omni Microphone." https://earthworksaudio.com/wp-content/uploads/2018/07/M30BX-Data- Sheet-2018.pdf

[21] H. Tokuno, O. Kirkeby, P. Nelson, "Inverse filter of sound reproduction systems using regularization" IEICE Transactions on Fundamentals of Electronics, Communications and Computer Sciences, Vol. 80, No. 5. 809-820. (1997).

[22] Middlicott, C; AES 147 Appendix (Addition Figures) https://www.charlesmiddlicott.co.uk/AES147

[23] Heller, A.J; Benjamin, E. M; Calibration of Soundfield Microphones using the Diffuse-Field Response. In Audio Engineering Society Convention 133, 8711, 2012.

[24] J, Daniel. “Représentation de champs acoustiques, application à la transmission et à la reproduction de scènes sonores complexes dans un contexte multimedia” PhD Thesis (2000)